Free Radical Research, June 2006; 40(6): 619–630

Turning point in apoptosis/necrosis induced by hydrogen peroxide

YOSHIRO SAITO[1], KEIKO NISHIO[1], YOKO OGAWA[1], JUNKO KIMATA[1,2], TOMOYA KINUMI[1], YASUKAZU YOSHIDA[1], NORIKO NOGUCHI[3,4], & ETSUO NIKI[1]

[1]*National Institute of Advanced Industrial Science and Technology (AIST), Human Stress Signal Research Center (HSSRC), Ikeda, Osaka 563 8577, Japan,* [2]*Thermo Electron KK, Yokohama, Japan,* [3]*Laboratory of Systems Biology and Medicine, Research Center for Advanced Science and Technology, University of Tokyo, Tokyo, Japan, and* [4]*Department of Environmental Systems Science, Faculty of Engineering, Doshisha University, Kyoto 610 0321, Japan*

Accepted by Professor N. Taniguchi

(Received 6 February 2006)

Abstract

The turning point between apoptosis and necrosis induced by hydrogen peroxide (H_2O_2) have been investigated using human T-lymphoma Jurkat cells. Cells treated with 50 μM H_2O_2 exhibited caspase-9 and caspase-3 activation, finally leading to apoptotic cell death. Treatment with 500 μM H_2O_2 did not exhibit caspase activation and changed the mode of death to necrosis. On the other hand, the release of cytochrome *c* from the mitochondria was observed under both conditions. Treatment with 500 μM H_2O_2, but not with 50 μM H_2O_2, caused a marked decrease in the intracellular ATP level; this is essential for apoptosome formation. H_2O_2-reducing enzymes such as cellular glutathione peroxidase (cGPx) and catalase, which are important for the activation of caspases, were active under the 500 μM H_2O_2 condition. Prevention of intracellular ATP loss, which did not influence cytochrome *c* release, significantly activated caspases, changing the mode of cell death from necrosis to apoptosis. These results suggest that ATP-dependent apoptosome formation determines whether H_2O_2-induced cell death is due to apoptosis or necrosis.

Keywords: *Apoptosis, necrosis, hydrogen peroxide, ATP, oxidative stress, apoptosome*

Abbreviations: *3-ABA, 3-aminobenzamide, AcOr, acridime orange, Apaf-1, apoptotic protease activating factor-1, cGPx, cellular glutathione peroxidase, 2D gel, two-dimentinal gel, GSH, glutathione, H_2O_2, hydrogen peroxide, PARP, poly (ADP-ribose) polymerase, pI, isoelectric point, PI, propidium iodide, Prx, peroxiredoxin, PS, phosphatidylserine, ROS, reactive oxygen species*

Introduction

The two forms of cell death, namely, apoptosis and necrosis, are distinguished on the basis of morphological and biochemical features [1]. Apoptosis is defined as the regulated, physiological type of death wherein the organism eliminates senescent, abnormal and potentially harmful cells [2]. In contrast, necrosis is described as a passive, nonphysiological type of death that is caused by accidental and acute damage to cells. Necrosis is characterized by cell swelling and disruption of the cell membrane, leading to the release of cellular contents; this may result in an inflammatory response [3,4]. In practical terms, apoptosis is clearly more advantageous to the organism since it eliminate dying cells by phagocytosis, thus preventing the release of intracellular contents and damage of the surrounding tissues.

"Oxidative stress" is defined as a disturbance in the oxidant–antioxidant balance in favor of the former [5]. Accumulating evidences suggest that oxidative

Correspondence: Y. Saito, National Institute of Advanced Industrial Science and Technology (AIST), Human Stress Signal Research Center (HSSRC), 1-8-31 Midorigaoka, Ikeda, Osaka 563 8577, Japan. Tel: 81 72 751 8293. Fax: 81 72 751 9964. E-mail: yoshiro-saito@aist.go.jp

ISSN 1071-5762 print/ISSN 1029-2470 online © 2006 Taylor & Francis
DOI: 10.1080/10715760600632552

damage of lipids, proteins and DNA potentially lead to degenerative diseases, such as atherosclerosis, cancer and neurodegenerative diseases and can also play a role in the aging process. To eliminate deleterious reactive oxygen species (ROS), cells possess an antioxidant system that is composed of numerous antioxidants with different molecular weights, solubilities and localizations in the cellular organelles [6,7]. Hydrogen peroxide (H_2O_2), which is possibly one of the most abundant ROS, plays a variety of roles in the body including those of a signaling molecule, an intermediate in metabolism and a cytotoxic agent in host defense and pathology [8]. H_2O_2 can be produced directly or indirectly (after the dismutation of superoxide) by NADPH oxidase and metabolic oxidases located in the mitochondrial respiratory chain. Cellular glutathione peroxidase (cGPx) and catalase are considered to function as major players in the regulation and/or elimination of the effects of H_2O_2 [9]. Peroxiredoxins (Prxs) are also a family of peroxidases that reduce H_2O_2 by using reducing equivalents that are provided by thiol-containing proteins such as thioredoxin [10].

A moderate concentration of H_2O_2 has been reported to trigger apoptosis, while an elevated concentration of H_2O_2 causes necrotic cell death [8,11–13]. As an apoptosis inducer, it has been reported that H_2O_2 can induce the release of cytochrome *c* that forms a complex with apoptotic protease-activating factor-1 (Apaf-1) [14]. When the nucleotide dATP or ATP binds to the Apaf-1-cytochrome *c* complex, it triggers its oligomerization to form an apoptosome [14,15]. The apoptosome recruits procaspase-9 and subsequently, procaspase-9 undergoes autocatalysis to yield active caspase-9 that in turn activates caspase-3 [15]. Activated caspase-3 cleaves cytoplasmic filaments, nuclear proteins and enzymes responsible for DNA metabolism and repair and subsequently causes downstream events such as chromatin fragmentation and phosphatidylserine (PS) externalization [14]. On the other hand, H_2O_2 might induce necrosis by preventing caspase activation or by directly inhibiting caspase activity [16–18]. It is thought that cellular ATP content is the key determinant in the selection between apoptosis and necrosis [3,4]. It is also known that some ATP-dependent steps are involved in the execution of apoptosis; for example, active nuclear transport, kinases and PS translocase are ATP-dependent, in addition to the formation of the apoptosome [4]; however, the details of the inhibition point in the apoptosis pathway and mechanism of necrosis remain to be elucidated.

The present study was carried out in order to elucidate the turning point and the key step between apoptosis and necrosis induced by H_2O_2. We characterized the timing of cell death, cytochrome *c* release, caspase activation, ATP loss and the alteration of the antioxidant system induced by different concentrations of H_2O_2.

Materials and methods

Chemicals

RPMI-1640 medium, *tert*-butyl hydroperoxide and GSH were obtained from Nacalai, Kyoto, Japan; GSH reductase from Oriental Yeast Co., Ltd., Tokyo, Japan; 3-aminobenzamide (3-ABA) from Sigma-Aldrich Co., St Louis, MO; H_2O_2 from Wako, Osaka, Japan; rabbit anti-caspase-3 and caspase-9 polyclonal antibody (pAb) from Cell Signaling Technology Inc., Beverly, MA; mouse anti-actin monoclonal antibody (mAb) (clone C4) from Chemicon International Inc., Temecula, CA; and mouse anti-cytochrome *c* mAb (BV-3026-3) was obtained from Medical & Biological Laboratories Co. Ltd., Nagoya, Japan. Rabbit anti-peroxiredoxin 2, 3, 4 and 6 pAbs were obtained from Lab Frontier, Seoul, Korea. Goat anti-DJ-1 pAb was purchased from Abcam, Inc., Cambridge, MA. Other chemicals were of the highest quality commercially available.

Cell culture and determination of apoptosis and necrosis

Jurkat E6-1 cells, human T-leukemia (American Tissue Type Collection, Manassas, VA), were maintained in RPMI-1640 medium containing 100 U/ml penicillin G, 100 μg/ml streptomycin, 0.25 μg/ml amphotericin B and 10% heat-inactivated fetal calf serum at 37°C under an atomosphere of 95% air and 5% CO_2. Cell viability was assessed by trypan blue dye (Gibco BRL, Rockville, MD) exclusion prior to all treatments and Jurkat cells with approximately 95% viability were employed. The cells were seeded at 5×10^5 cells/ml and treated with H_2O_2 for indicated time.

PS exposure was measured by the binding of annexin V-FITC according to the protocol outlined by the manufacture in the Apoptosis Detection-kit (Medical & Biological Laboratories) [19]. Treated cells were stained with annexin V-FITC and propidium iodide (PI), followed by analysis with a Cytomics FC500 Flow Cytometry System (Beckman Coulter, Inc., Miami, FL) with a 488 nm argon laser. Data were collected from 10,000 events.

To confirm the changes in nuclear morphology, acridine orange (AcOr)/ethidium bromide (EtBr) staining was conducted [20]. Aliquots of treated cells were centrifuged and resuspended in 25 μl of PBS, to which 1 μl of dye mix (100 μg/ml AcOr and 100 μg/ml EtBr in PBS) was added. The cells were visualized under a fluorescence microscope IX 70 (Olympus Co., Tokyo Japan), using U-MWB2 filter.

Caspase activity assays

Caspase activity was measured by cleavage of the Asp–Glu–Val–Asp (DEVD) and Leu–Glu–His–Asp (LEHD) peptide-conjugated *p*-nitroanilide (*p*NA), according to the protocol outlined by the manufacturer of the Caspase-3/CPP32 colorimetric protease assay

kit and Caspase-9/Mch 6 protease assay kit (Medical & Biological Laboratories), respectively [21]. Substrate cleavage, which resulted in the release of *p*NA (405 nm), was measured using a Multiskan Ascent plate reader (Thermo Labsystems, Helsinki, Finland). Absorbance units were converted to *p* moles of *p*NA using a standard curve generated with free *p*NA.

Protein assay

The protein concentration was determined by using the BCA protein assay kit (Pierce Biotechnology, Inc., Rockford, IL) with bovine serum albumin as a standard.

Protein extraction, subcellular fractionation and Western blot analysis

To obtain total cell extracts, treated cells were corrected, washed with ice-cold PBS and resuspended at 4°C for 30 min in lysis buffer [150 mM NaCl, 50 mM Tris–HCl, pH 7.4, 50 mM NaF, 5 mM EDTA, 0.5% Triton X-100 and 1 mM Na_3VO_4 with a protease inhibitor cocktail tablet (Roche Diagnostics, Penzberg, Germany)]. Nuclei and unlysed cellular debris were removed by centrifugation at 800*g* for 10 min. Equal amounts of protein (from 10 to 50 μg) were loaded and separated by sodium dodecyl sulphate–polyacrylamide gel electrophoresis (SDS–PAGE).

The amount of cytochrome *c* released from the mitochondrial intermembrane space into the cytosol was determined by digitonin permeabilization [22]. Treated cells were washed with ice-cold PBS and resuspended at 4°C for 5 min in permeabilization buffer containing 75 mM NaCl, 1 mM NaH_2PO_4, 8 mM Na_2PO_4, 250 mM sucrose, a protease inhibitor cocktail tablet (Roche Diagnostics) and 0.05% digitonin. Following a centrifugation step at 800*g* at 4°C for 10 min, the supernatant was separated from the pellet consisting of mitochondrial and cellular debris. The supernatant containing cytoplasmic proteins was purified by centrifugation at 13,000*g* at 4°C for 10 min. Equal amounts of protein were loaded on separated by SDS–PAGE.

In all cases, the detection of specific proteins either in the total cell extracts or in the cell fractions was carried out by Western blot analysis, following the previously described procedure [23].

Measurement of intracellular ATP

The cellular ATP content was determined using a bioluminescent somatic cell assay kit according to the manufacture's instructions (Sigma) [24]. The ATP content was measured with the luciferin/luciferase method in MiniLumat LB9506 luminometer (Berthold Technologies, Wildbad, Germany). The absolute values of ATP content were determined using an internal ATP standard.

Hydrogen peroxide consumption

H_2O_2 concentrations were measured using the ferrous oxidation of xylenol orange (FOX) assay [25]. At specific intervals, the cells were pelleted and supernatants were added to the FOX reagent consisting of 100 μM xylenol orange, 250 μM ammonium ferrous sulfate, 100 mM sorbitol and 25 mM H_2SO_4. An increase in A560 nm was measured and concentration was calculated with a standard curve generated with reagent H_2O_2.

Measurement of antioxidant enzyme

To measure cellular GPx (cGPx) activity, a coupled enzyme assay, which was performed by following the oxidation of NADPH, was used as described previously [26]. Cytosol fraction for cGPx assay was prepared as described previously [27]. The assay conditions were as follows: 0.1 M Tris–HCl; pH 8.0; 0.2 mM NADPH; 0.5 mM EDTA; 1 mM NaN_3; 2 mM GSH; 1 U/ml of GSH reductase; and 70 μM *tert*-butyl hydroperoxide. The oxidation of NADPH was followed at 340 nm at 37°C and the activity was expressed as *n* moles of NADPH oxidized per minute.

Catalase activities were examined according to the protocol outlined by the manufacturer of catalase assay kit (Cayman Chemical Co., Ann Arbor, MI) [28].

Two-dimensional gel electrophoresis

After treatment with H_2O_2, the cells were washed with PBS and then dissolved in isoelectric focusing sample buffer consisting of 9 M urea, 2% {3-[(3-cholamidopropyl)dimetylammonio]-1-propanesulphonate} (Chaps), 65 mM dithioerythritol (DTE) and 0.5% carrier ampholyte (pH 4–7; Amersham Biosciences), as described previously [29]. The sample solution (50 μg protein) was applied to an immobilized pH gradient gel (7 cm, pH 4–7; Amersham Biosciences) and rehydrated for 12 h. Isoelectric focusing was performed for a total of 16,750 Vh at a maximum voltage of 5000 V. Each strip was equilibrated in 50 mM Tris–HCl (pH 8.8), 6 M urea, 2% SDS, 30% glycerol and 20 mM DTE for 20 min. The second dimension was carried out by 12.5% SDS–PAGE. Proteins separated by 2D gel were transferred to polyvinylidene fluoride (PVDF) membrane (Millipore Co., Bedford, MA) and subsequently subjected to Western blot analysis described above.

Stastical analysis

Statistical analyses were performed on a Microsoft personal computer by an analysis of variance using Dunnett and Tukey test for multiple comparisons

(ANOVA). The calculation method was shown in the each figure legend. Data were expressed mean values ± SD.

Results

Apoptotic and necrotic cell death induced by H_2O_2

We first analyzed the generation of apoptosis and necrosis in Jurkat cells treated with different concentrations of H_2O_2. For quantification, the rate of apoptosis and necrosis were determined by determining the frequency of cells that demonstrated PS exposure and free penetration of PI (Figure 1(a)). Characteristic morphological changes that are observed during apoptosis (condensed/fragmented chromatin) and necrosis (normal chromatin distribution), were also confirmed using AcOr and EtBr (Figure 1(b)). A dose-dependent study revealed that

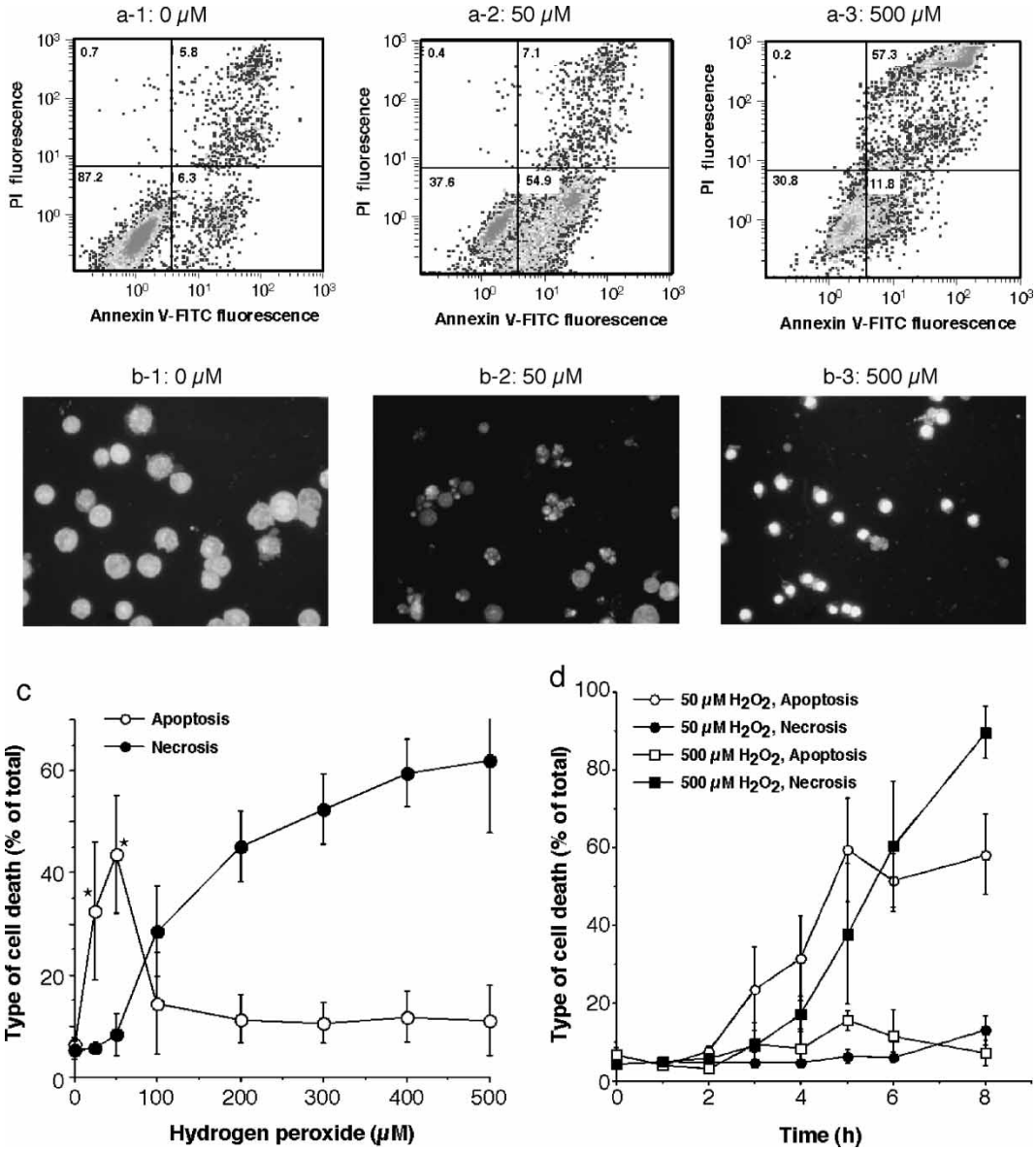

Figure 1. H_2O_2-induced apoptosis and necrosis. (a) The cells (5×10^5 cells/ml) were treated with 0, 50 and 500 μM of H_2O_2 for 6 h. Subsequently, the cell samples were treated with annexin V-FITC and PI and were subjected to flow cytometry. The data patterns shown here are representatives of three experiments. The percentages of cells are shown in the left corner in each class. (b) The cells treated with H_2O_2 for 6 h were stained with AcOr and EtBr and viewed under the fluorescence microscope. (c) The cells were treated with variable amounts of H_2O_2 for 6 h and then subjected to flow cytometry. The percentages of apoptosis (annexin V-FITC positive and PI negative) and necrosis (PI positive) with SD of at least three experiments are shown. *, $p < 0.05$ when compared with 0 μM H_2O_2 (Dunnett, ANOVA). In the case of necrosis, the statistical significance of differences ($p < 0.05$) between 0 μM H_2O_2 and each point were observed above 100 μM H_2O_2. (d) The cells were incubated with 50 or 500 μM H_2O_2 for indicated time periods and then subjected to flow cytometry. The percentages of apoptosis and necrosis with SD of at least three experiments are shown. In the case of apoptosis with 50 μM H_2O_2, the statistical significance ($p < 0.05$) of differences between time zero and each point were observed above 3 h (Dunnett, ANOVA). In the case of necrosis with 500 μM H_2O_2, the statistical significance ($p < 0.05$) of differences were observed above 4 h of the incubation period.

treatment with 50 μM H_2O_2 for 6 h incubation caused only apoptosis, while the rate of necrosis increased when treated with H_2O_2 at a concentration of 100 μM or more; this rate reached a plateau at 500 μM H_2O_2 (Figure 1(c)). We, therefore, used 50 and 500 μM H_2O_2 for induction of apoptosis and necrosis, respectively. A time-dependent study revealed that apoptosis and necrosis occurred independently at each concentration (Figure 1(d)) and that apoptosis-derived secondary necrosis might not have occured during this 8 h treatment.

Characterization of caspase activation under the apoptosis and necrosis-inducing condition

Since 77% of apoptosis induced by H_2O_2 was suppressed in the presence of the caspase inhibitor VAD–FMK (20 μM, data not shown), we focused on the caspase cascade, which is required for the execution of the intrinsic pathway of apoptosis. Extracts from cells treated with 50 μM of H_2O_2 for 6 h exhibited a marked increase in DEVDase (indicative of caspase-3; Figure 2(a-1)) and LEHDase (indicative of caspase-9; Figure 2(b-1)) activities. However, a significant increase in these activities was not observed in cells treated with 500 μM H_2O_2 during the necrosis-inducing condition. In order to confirm the proteolytic activation of caspases, Western blot analysis was conducted using specific antibodies against caspase-3 and caspase-9. Therefore, cleaved and activated caspase-3 and caspase-9 were only observed in cell extracts that were treated with 50 μM H_2O_2 during the apoptosis-inducing condition; these were not observed with 500 μM H_2O_2 during the necrosis-inducing condition at any time during the examination (Figure 2(a-2),(b-2)). These results suggest that caspase-3 and caspase-9 are not activated under the necrosis-inducing condition.

Dose-dependent release of cytochrome c *from mitochondria*

The release of the cytochrome *c* from the mitochondria to the cytosol is required for the assembly of the apoptosome and hence, for the activation of the caspase cascade in the intrinsic pathway of apoptosis [14]. Western blot analyses were carried out to detect

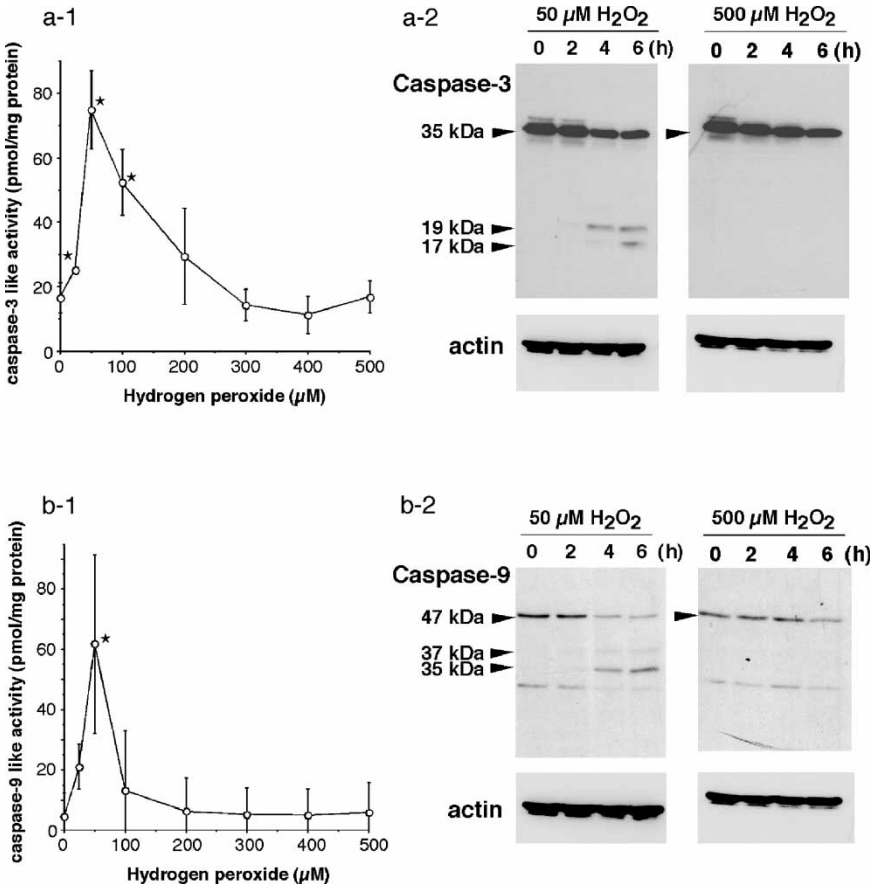

Figure 2. Caspase activities under the apoptosis- and necrosis-inducing conditions. Samples were taken after the cells were treated with variable amounts of H_2O_2 for 6 h and the caspase activity was measured using DEVD-*p*NA (a-1) or LEHD-*p*NA (b-1) as a substrate. The mean and SD of at least three experiments has been shown. *, $p < 0.05$ when compared with 0 μM H_2O_2 (Dunnett, ANOVA). (a-2, b-2) The cell samples (20 μg protein per lane) treated with 0, 50 and 500 μM H_2O_2 for indicated time period were subjected to Western blot analysis using an antibody against caspase 3 (a-2) or caspase 9 (b-2).

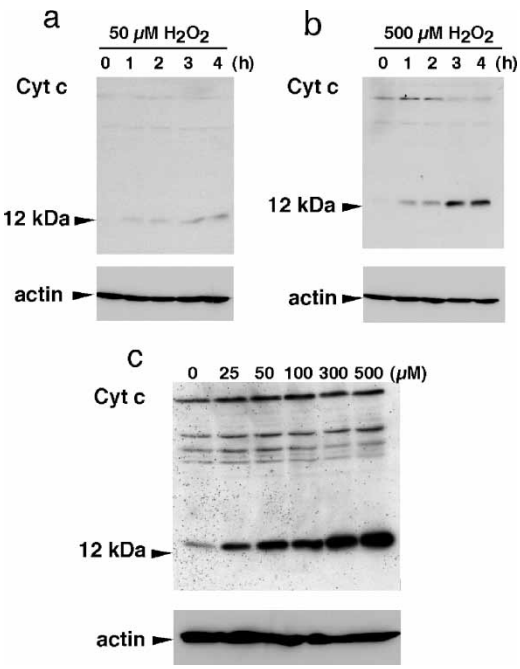

Figure 3. Cytochrome *c* release. Cytosolic extracts (10 μg protein per lane) obtained from the cells treated with 50 μM: (a) or 500 μM; (b) H_2O_2 for indicated time periods; and from the cells treated with variable amounts of H_2O_2 for 2 h were used for Western blot analysis.

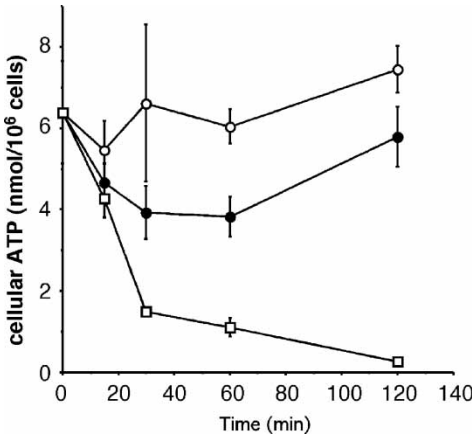

Figure 4. Alteration in the ATP level. ATP content in the cells treated with 0 μM (open circle), 50 μM (closed circle) or 500 μM (open square) H_2O_2 for indicated time periods were determined. The mean and SD of at least three experiments are shown.

the presence of cytochrome *c* in cytosolic extracts from cells treated with 50 and 500 μM of H_2O_2. As shown in Figure 3, cytochrome *c* could be detected in extracts from cells treated with both 50 and 500 μM H_2O_2, which caused apoptosis and necrosis, respectively. The time-dependent study revealed that cytosolic cytochrome *c* was detectable after an incubation of 1 h during both the conditions and its levels increased after 3 h of the H_2O_2 treatment. The dose-dependent study revealed that the release of cytochrome *c* from mitochondoria was dose-dependent; this was not the case with PS exposure and caspase activation. Thus, it was considered that the mitochondria-dependent apoptotic pathway was arrested after cytochrome *c* release and prior to caspase-9 activation during necrotic cell death that was induced by 500 μM H_2O_2.

Depletion of ATP levels under the necrosis-inducing condition

Apoptosis involves energy-requiring steps. One of which is the formation of the protein complex, namely apoptosome, between Apaf-1 and cytochrome *c* [14,15]. Thus, an experiment was carried out to compare the alterations in the ATP levels on treatment with H_2O_2. As shown in Figure 4, treatment with 50 μM H_2O_2 caused a slight decrease in the ATP level; these values recovered to a value close to the control value at 120 min. On the other hand, treatment with 500 μM H_2O_2 caused a rapid and profound depletion of ATP; the ATP level reached 23% that of the control cells at 30 min. More than 95% loss of intracellular ATP was observed within 120 min under the necrosis-inducing condition.

Characterization of the antioxidant status under the apoptosis- and necrosis-inducing conditions

It has been reported that the active site cysteine residues of caspases are susceptible to oxidation, resulting in caspase inactivation and thus, the potential inhibition of apoptosis [4,16]. In order to understand the cellular redox status, we analyzed the antioxidant capacity under oxidative stress induced by H_2O_2. The activities of H_2O_2-removing enzymes, such as cGPx and catalase, did not changed under the apoptosis-inducing condition and their activities were also detected at 120 min after the addition of 500 μM H_2O_2 (Figure 5(a),(b)). It was observed that total GSH and oxidized GSH remained unchanged until 60 min of the incubation period (data not shown). Further, the oxidation of Prxs, other H_2O_2-reducing enzymes and the antioxidant protein DJ-1 were examined for proteins obtained from Jurkat cells that were exposed to H_2O_2 by Western blot analysis combined with two-dimensional gel electrophoresis (2D gel). As shown in Figure 6, the acidic spot shift of these proteins occurred 15 or 30 min after H_2O_2 exposure. The acidic spot shifts of Prx 2, 3, and 6 were observed under apoptosis- and necrosis-inducing conditions, while Prx 4 and DJ-1 shifted only under the necrosis-inducing condition. It has been demonstrated that these acidic pI shifts are due to a post translational process that is caused by the oxidation of a cysteine residue to cysteine sulphinic acid

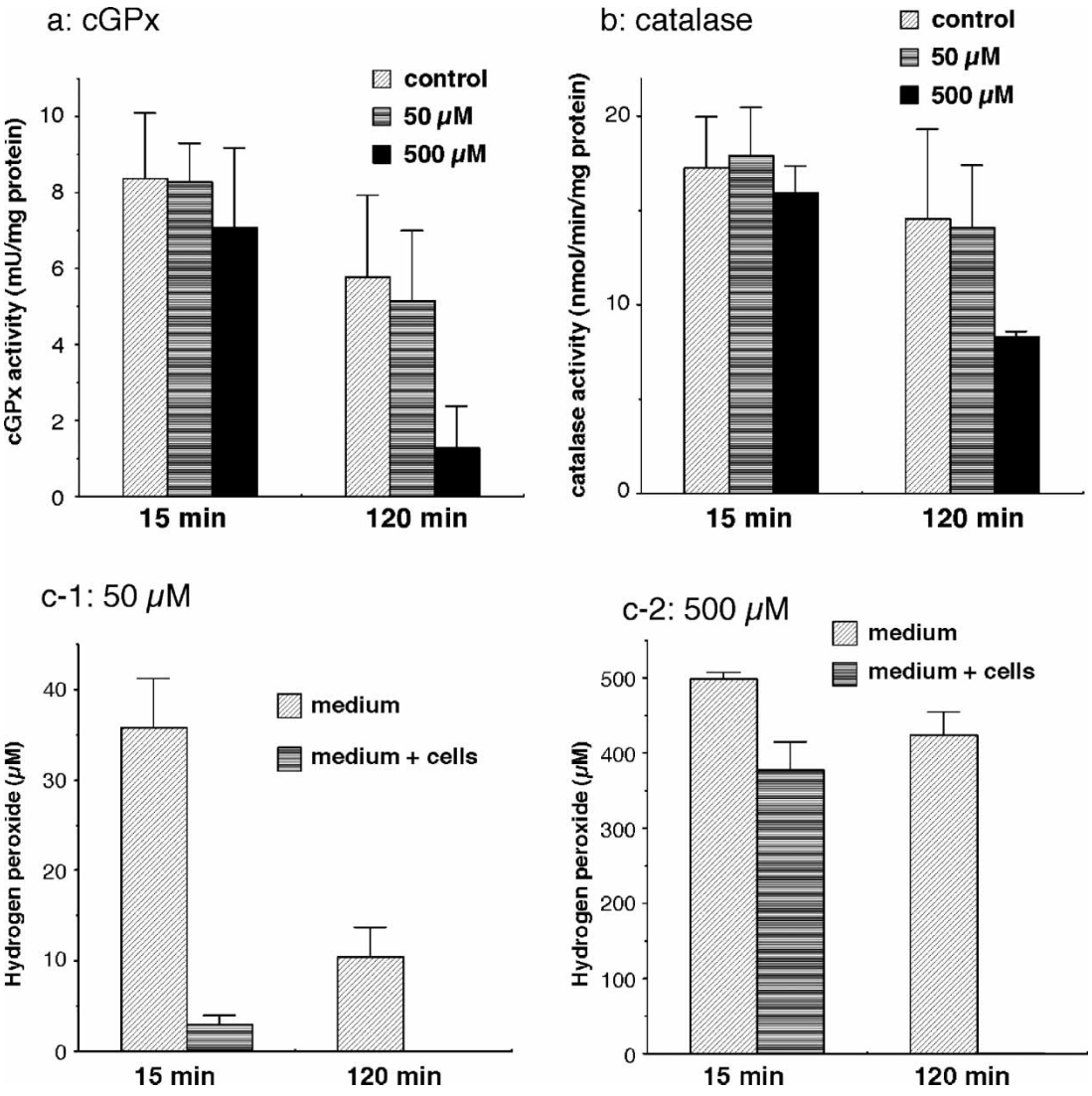

Figure 5. Antioxidant enzyme activities and H_2O_2 consumption. (a,b) Cells were treated with 0, 50 and 500 μM H_2O_2 for the indicated time periods and activities of selenoenzyme cGPx (a) and catalase (b) were measured. The enzyme activities in each cell sample are shown as means ± SD. The consumption of 50 μM (c-1) and 500 μM (c-2) H_2O_2 with or without cells for indicated time periods was determined. The mean and SD of at least three experiments are shown.

(Cys-SO_2H) or cysteine sulphonic acid (Cys-SO_3H); these are inactivated forms of Prxs [29,30]. Thus, these results suggest that Prxs were immediately oxidized and inactivated under the conditions of oxidative stress, which were generated by the exposure of the cells to H_2O_2. We also examined the pI shift of caspase-3 under apoptosis- and necrosis-inducing conditions; however, no significant change was observed (data not shown).

To confirm the working of the cellular H_2O_2-removing system, we measured the H_2O_2 content in the cell culture medium. As shown in Figure 5(c-1), most of the H_2O_2 disappeared within 15 min from the medium under apoptosis-inducing condition. In the case of the necrosis-inducing condition, 80% of the H_2O_2 remained in the culture medium even at 15 min; however, it disappeared after incubation for 120 min.

Effect of poly (ADP-ribose) polymerase inhibitor on ATP loss and mode of cell death

To clarify the role of the ATP-dependent step in the regulation of H_2O_2-induced apoptosis or necrosis, we examined the effect of the poly (ADP-ribose) polymerase (PARP) inhibitor, namely, 3-ABA. This agent has been reported to preserve the ATP pool in cells treated with DNA-damaging agents, including H_2O_2, thus preventing the occurrence of necrosis resulting from severe ATP depletion [31,32]. It was observed that in the presence of 3-ABA, the ATP loss induced by 500 μM H_2O_2 was prevented (Figure 7(a))

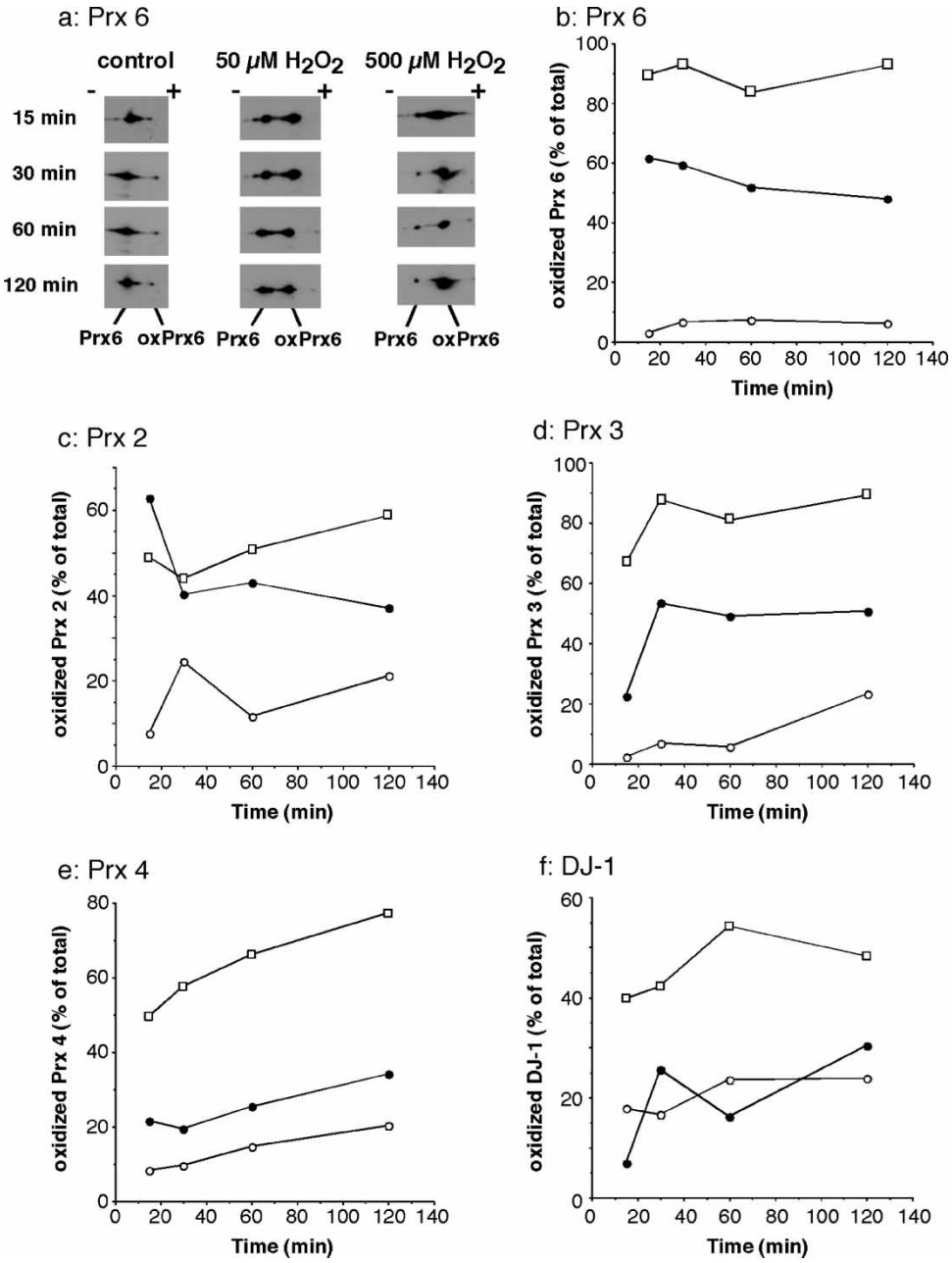

Figure 6. Western blot analysis of 2D gel separated proteins. Cell samples (50 μg protein) obtained from the cells treated with 0 μM (open circle), 50 μM (closed circle) and 500 μM H_2O_2 (open square) for indicated time periods were separated by 2D gel electrophoresis and subsequently subjected to Western blot analysis using antibodies specific to each protein shown in the left corner. (a) Prx 6 spots were detected with a Prx 6-specific polyclonal antibody. (b) The intensities of the spots of oxidized Prx 6 (acidic spot) and Prx 6 were measured. The relative ratio of oxidized Prx 6 was calculated and plotted. (c–f) Relative intensities of the acidic spots were shown. The acidic spot shift of these proteins in Jurkat cells treated with H_2O_2 for 2 h was also confirmed by 2D gels visualized by fluorescent staining ($n = 3$).

and that the mode of cell death switched completely from necrosis to apoptosis under the 500 μM H_2O_2 necrosis-inducing condition (Figure 7(b)). Further, the mitochondria-dependent apoptotic pathway was investigated in the treatment with both 3-ABA and 500 μM H_2O_2. Cytochrome *c* release was not influenced by cotreatment with 3-ABA and 500 μM H_2O_2 (Figure 8(a)), while caspase-3 and caspase-9 demonstrated significant activities under coexistence (Figure 8(b)). Cleaved and activated caspase-3 and caspase-9 were observed in cell extracts treated with both 3-ABA and 500 μM H_2O_2; this was in accordance with their enzyme activities.

Discussion

It is well known that a moderate concentration of H_2O_2 has been reported to trigger apoptosis, while an elevated concentration of H_2O_2 causes necrotic cell death [8,11–13]. Understanding the mechanism of

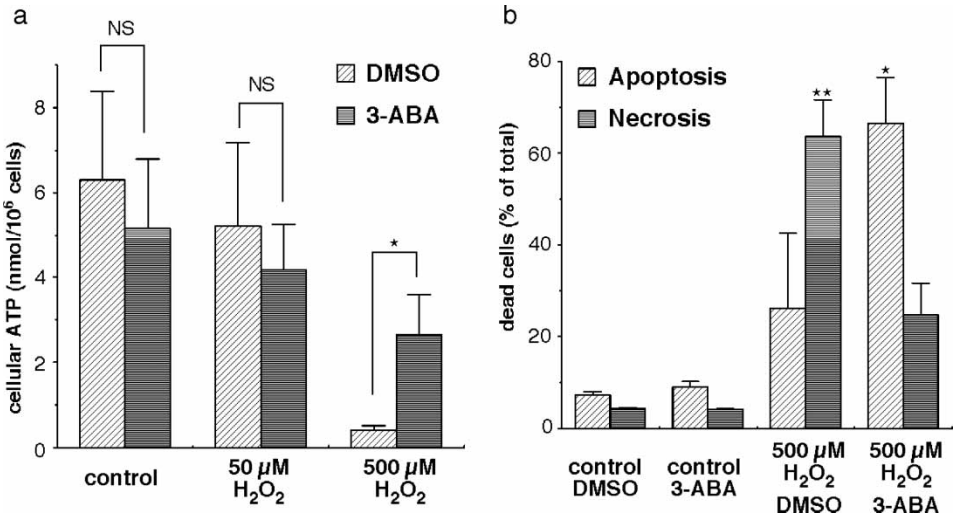

Figure 7. Modulation in the ATP level and the mode of cell death by using 3-ABA. After incubation with 2.5 mM 3-ABA or control DMSO for 5 min, the cells were treated with 0, 50 and 500 μM H_2O_2. (a) Two hours after H_2O_2 exposure, the cellular ATP content was determined. The mean and SD of at least three experiments are shown. *, $p < 0.05$ (Tukey, ANOVA). NS, not significant. (b) Six hours after H_2O_2 exposure, flow cytometry using annexin V-FITC and PI was performed. The percentages of apoptosis and necrosis with SD of at least three experiments are shown. *, $p < 0.05$ when compared with apoptosis observed in DMSO and 3-ABA groups (Tukey, ANOVA). **, $p < 0.05$ when compared with necrosis observed in DMSO and 3-ABA groups (Tukey, ANOVA).

necrosis is important, especially for pathology to prevent an inflammation and damage of the tissues. It has been reported, cellular ATP content is the key determinant in the selection between apoptosis and necrosis [3,4]. However, the key ATP-dependent step in the execution of necrosis or inhibition of apoptosis has not yet been elucidated. In the present study, using Jurkat cells, we observed that apoptosis and necrosis occurred independently at different H_2O_2 concentrations (Figure 1(d)). Therefore, it is considered that this is a suitable experimental model that can be used to clarify the turning point in H_2O_2-induced apoptosis and necrosis.

We observed that caspase inhibitor almost completely blocked the apoptosis induced by H_2O_2. This observation suggests that activation of caspase is the key determinant in the execution of apoptosis induced by H_2O_2. It has been demonstrated that the caspase cascades can be activated and amplified after the release of cytochrome *c* from the mitochondria into the cytosol during the early stages of apoptosis [14,33]. Cytosolic cytochrome *c* binds to Apaf-1, a cytosolic protein containing a caspase recruitment domain (CARD) and a nucleotide-binding domain. Apaf-1 alone binds the nucleotide dATP or ATP poorly; however, the binding of cytochrome *c*, which is independent of the presence of nucleotides, increases Apaf-1 affinity for dATP/ATP [15]. It has been reported that the binding of a nucleotide to the Apaf-1/cytochrome *c* complex triggers its oligomerization to form the apoptosome, a multimeric Apaf-1 and cytochrome *c* complex [14,15,33]. In the present study, when cytochrome *c* was released under the H_2O_2-induced necrotic condition, the cellular ATP level decreased severely. Thus, it was considered that the binding of the nucleotide to the Apaf-1/cytochrome *c* complex was hindered and the amplification of caspase cascade was arrested under the necrosis-inducing condition.

In order to elucidate that the ATP-requiring step between cytochrome *c* release and caspase-9 activation functions as a turning point in H_2O_2-induced apoptosis or necrosis, the cellular redox status, which is important for the activation of caspases and the execution of apoptosis, was characterized. The active site cysteine residue of caspase is susceptible to oxidation [34], which in turn results in caspase inactivation and thus potential inhibition of apoptosis. It is known that various oxidants with different structures, solubilities and reactivities, cause different types of oxidative stress. In the case of nitric oxide (NO), it has been reported that apoptosis is regulated by S-nitrosation of the caspase cysteine residue [35]. On the other hand, it has been demonstrated that H_2O_2 reversibly inactivates caspases and that antioxidants both prevent and reversed H_2O_2-induced inactivation [18]. As shown in Figure 5, the enzyme activities of H_2O_2-removing system are detected even during necrosis, although these enzyme activities significantly decrease within 2 h of the incubation period. We also observed that the total GSH and oxidized GSH remained unchanged for 1 h of the incubation period during the necrosis-inducing condition (data not shown). Therefore, it is thought that the H_2O_2-reducing system is active during H_2O_2-induced necrotic condition. Infact, we observed that

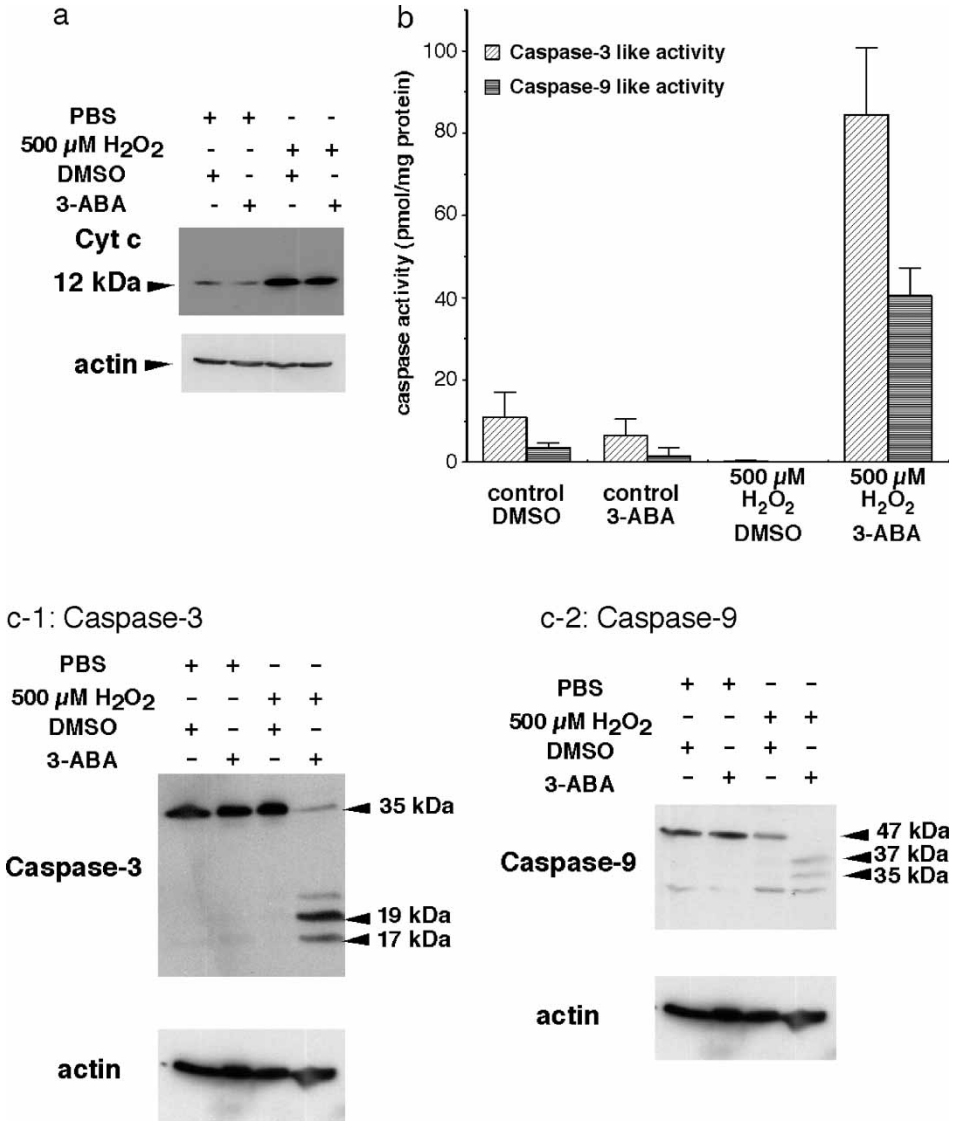

Figure 8. Effect of 3-ABA on cytchrome *c* release and caspase activation. After incubation with 2.5 mM 3-ABA or control DMSO for 5 min, the cells were treated with or without 500 μM H_2O_2. (a) Two hours after H_2O_2 exposure, the cytosolic extracts (20 μg protein per lane) obtained from treated cells were used for Western blot analysis. (b,c) Six hours after H_2O_2 exposure, cell samples obtained from treated cells were used for measurement of caspase activity (b) or Western blot analysis (c). The mean and SD of at least three experiments are shown.

exogenous 500 μM H_2O_2 was clearly eliminated due to the presence of cells at 2 h of the incubation period (Figure 5(c)).

We observed that Prxs and DJ-1 were highly oxidized in a dose-dependent manner under the oxidative stress induced by H_2O_2 (Figure 6). Compared with cGPx and catalase, the H_2O_2-reducing system that is composed of Prxs appears to be sensitive and can be easily damaged by oxidative stress. In the case of Prxs, it has been reported that the active site cysteine can be irreversibly oxidized by peroxide for reducing equivalents provided by thiol-containing proteins, such as thioredoxin; however, this oxidation is reversible for the ATP-dependent enzyme sulfiredoxin (Srx) [10,36,37]. Further, it has been reported that this ATP-dependent process is specific for 2-Cys Prx isoforms such as Prx 2, 3, and 4 that were analyzed in this study [38]. Interestingly, it was observed that the amount of oxidized Prx 2 has a tendency to decrease only under the apoptosis-inducing condition (Figure 6(c)), in which the ATP level was maintained close to the control level. Since Srx is restricted to the cytosol [37], it is reasonable that cytosolic Prx 2 is reduced, but Prx 3 and Prx 4, which are located in the mitochondria and the endoplasmic reticulum, respectively, are not reduced. We have previously reported that Cys-106 of DJ-1 is the most sensitive to oxidative stress among three cysteine residues [29]. In this experiment, using exogenous H_2O_2, we proved that the susceptibility of DJ-1 to oxidation is relatively low; this was in accordance with our previous observation using HUVEC cells [29]. In the case of cysteine protease caspase, the acidic spot shift was not observed (data not shown). Therefore, it

appears that the active site cysteine residue of caspase-3 is not oxidized to Cys-SO_2H or Cys-SO_3H.

The treatment with the PARP inhibitor was effective against ATP loss and necrosis induced by 500 μM H_2O_2 (Figures 7, 8). Interestingly, the ratio of apoptosis induced by the cotreatment with 500 μM H_2O_2 and 3-ABA was higher than that observed in the case of 50 μM H_2O_2-induced apoptotic condition, which was 66.6 ± 9.9 and 43.7 ± 11.6% of the total cells, respectively (Figures 1(c), 7(b)). In accordance with this observation, a high ratio of the activated caspases to the intact form was observed with both 500 μM H_2O_2 and 3-ABA; this was not the case under the 50 μM H_2O_2 condition (Figures 2, 8). A significant increase in caspase activation is observed in the presence of both 500 μM H_2O_2 and 3-ABA; this might reflect an increased cytosolic cytochrome *c*, which was released from mitochondria in a dose-dependent manner.

In addition to the formation of the apoptosome, some other ATP-dependent steps are involved in the execution of apoptosis; for example, active nuclear transport mechanism, kinases and PS translocase are ATP-dependent [4]. Considering the suppressive effect of PARP inhibitor on ATP-loss induced by 500 μM H_2O_2, it is thought that PARP activation is one of the major cause for ATP-loss induced by H_2O_2. It is well known that PARP is a substrate for caspase-3 and that activated caspase-3 cleaves and inactivates PARP [39]. Since the reduction in the ATP level induces various dysfunctions such as prevention of apoptosis and elevation of lysosomal pH [3,4,40], inactivation of PARP by caspase-3 might play a role in saving cellular ATP required for other ATP-dependent steps mentioned above.

In conclusion, the present study demonstrated that 50 and 500 μM of H_2O_2 cause apoptosis and necrosis, respectively. A sequential apoptotic signal was observed during apoptosis, while an ATP-dependent step of the apoptotic pathway occurring between cytochrome *c* release and caspase-9 activation was arrested during necrosis. Considering the antioxidant status and suppressive effect of cellular ATP loss, it is considered that the ATP-dependent formation of the apoptosome functions as a turning point to determine H_2O_2-induced apoptotic and necrotic cell death.

References

[1] Wyllie AH, Kerr JF, Currie AR. Cell death: The significance of apoptosis. Int Rev Cytol 1980;68:251–306.

[2] Schwartz LM, Smith SW, Jones ME, Osborne BA. Do all programmed cell deaths occur via apoptosis? Proc Natl Acad Sci USA 1993;90:980–984.

[3] Leist M, Single B, Castoldi AF, Kuhnle S, Nicotera P. Intracellular adenosine triphosphate (ATP) concentration: A switch in the decision between apoptosis and necrosis. J Exp Med 1997;185:1481–1486.

[4] Nicotera P, Melino G. Regulation of the apoptosis–necrosis switch. Oncogene 2004;23:2757–2765.

[5] Sies H. Oxidative stress: From basic research to clinical application. Am J Med 1991;91:31S–38S.

[6] Halliwell B, Gutteridge JMC. Free radicals in biology and medicine. New York: Oxford University Press; 1999.

[7] Niki E, Yoshida Y, Saito Y, Noguchi N. Lipid peroxidation: Mechanisms, inhibition and biological effects. Biochem Biophys Res Commun 2005;338:668–676.

[8] Davies KJ. The broad spectrum of responses to oxidants in proliferating cells: A new paradigm for oxidative stress. IUBMB Life 1999;48:41–47.

[9] Dringen R, Pawlowski PG, Hirrlinger J. Peroxide detoxification by brain cells. J Neurosci Res 2005;79:157–165.

[10] Rhee SG, Chae HZ, Kim K. Peroxiredoxins: A historical overview and speculative preview of novel mechanisms and emerging concepts in cell signaling. Free Radic Biol Med 2005;38:1543–1552.

[11] Hampton MB, Orrenius S. Dual regulation of caspase activity by hydrogen peroxide: Implications for apoptosis. FEBS Lett 1997;414:552–556.

[12] Gardner AM, Xu FH, Fady C, Jacoby FJ, Duffey DC, Tu Y, Lichtenstein A. Apoptotic vs. nonapoptotic cytotoxicity induced by hydrogen peroxide. Free Radic Biol Med 1997;22:73–83.

[13] Lee YJ, Shacter E. Oxidative stress inhibits apoptosis in human lymphoma cells. J Biol Chem 1999;274:19792–19798.

[14] Wang X. The expanding role of mitochondria in apoptosis. Genes Dev 2001;15:2922–2933.

[15] Zou H, Li Y, Liu X, Wang X. An APAF-1.cytochrome *c* multimeric complex is a functional apoptosome that activates procaspase-9. J Biol Chem 1999;274:11549–11556.

[16] Samali A, Nordgren H, Zhivotovsky B, Peterson E, Orrenius S. A comparative study of apoptosis and necrosis in HepG2 cells: Oxidant-induced caspase inactivation leads to necrosis. Biochem Biophys Res Commun 1999;255:6–11.

[17] Lee YJ, Shacter E. Hydrogen peroxide inhibits activation, not activity, of cellular caspase-3 *in vivo*. Free Radic Biol Med 2000;29:684–692.

[18] Borutaite V, Brown GC. Caspases are reversibly inactivated by hydrogen peroxide. FEBS Lett 2001;500:114–118.

[19] Pigault C, Follenius-Wund A, Schmutz M, Freyssinet JM, Brisson A. Formation of two-dimensional arrays of annexin V on phosphatidylserine-containing liposomes. J Mol Biol 1994;236:199–208.

[20] Mukhopadhyay D, Sundereshan S, Rao C, Karande AA. Placental protein 14 induces apoptosis in T cells but not in monocytes. J Biol Chem 2001;276:28268–28273.

[21] Casciola-Rosen L, Nicholson DW, Chong T, Rowan KR, Thornberry NA, Miller DK, Rosen A. Apopain/CPP32 cleaves proteins that are essential for cellular repair: A fundamental principle of apoptotic death. J Exp Med 1996;183:1957–1964.

[22] Marques CA, Keil U, Bonert A, Steiner B, Haass C, Muller WE, Eckert A. Neurotoxic mechanisms caused by the Alzheimer's disease-linked Swedish amyloid precursor protein mutation: Oxidative stress, caspases and the JNK pathway. J Biol Chem 2003;278:28294–28302.

[23] Saito Y, Sato N, Hirashima M, Takebe G, Nagasawa S, Takahashi K. Domain structure of bi-functional selenoprotein P. Biochem J 2004;381:841–846.

[24] Borutaite V, Brown GC. Nitric oxide induces apoptosis via hydrogen peroxide, but necrosis via energy and thiol depletion. Free Radic Biol Med 2003;35:1457–1468.

[25] Wolf PS. Ferrous ion oxidation in presence of ferric ion indicator xylenol orange for measurement of hydroperoxides. Methods Enzymol 1994;233:182–189.

[26] Saito Y, Takahashi K. Characterization of selenoprotein P as a selenium supply protein. Eur J Biochem 2002;269: 5746–5751.
[27] Saito Y, Yoshida Y, Akazawa T, Takahashi K, Niki E. Cell death caused by selenium deficiency and protective effect of antioxidants. J Biol Chem 2003;278:39428–39434.
[28] Johansson LH, Borg LA. A spectrophotometric method for determination of catalase activity in small tissue samples. Anal Biochem 1988;174:331–336.
[29] Kinumi T, Kimata J, Taira T, Ariga H, Niki E. Cysteine-106 of DJ-1 is the most sensitive cysteine residue to hydrogen peroxide-mediated oxidation *in vivo* in human umbilical vein endothelial cells. Biochem Biophys Res Commun 2004;317:722–728.
[30] Wagner E, Luche S, Penna L, Chevallet M, Van Dorsselaer A, Leize-Wagner E, Rabilloud T. A method for detection of overoxidation of cysteines: Peroxiredoxins are oxidized *in vivo* at the active-site cysteine during oxidative stress. Biochem J 2002;366:777–785.
[31] Ha HC, Snyder SH. Poly(ADP-ribose) polymerase is a mediator of necrotic cell death by ATP depletion. Proc Natl Acad Sci USA 1999;96:13978–13982.
[32] Troyano A, Sancho P, Fernandez C, de Blas E, Bernardi P, Aller P. The selection between apoptosis and necrosis is differentially regulated in hydrogen peroxide-treated and glutathione-depleted human promonocytic cells. Cell Death Differ 2003;10:889–898.
[33] Adrain C, Martin SJ. The mitochondrial apoptosome: A killer unleashed by the cytochrome seas. Trends Biochem Sci 2001;26:390–397.
[34] Thornberry NA, Lazebnik Y. Caspases: Enemies within. Science 1998;281:1312–1316.
[35] Liu L, Stamler JS. NO: An inhibitor of cell death. Cell Death Differ 1999;6:937–942.
[36] Biteau B, Labarre J, Toledano MB. ATP-dependent reduction of cysteine–sulphinic acid by S. cerevisiae sulphiredoxin. Nature 2003;425:980–984.
[37] Chang TS, Jeong W, Woo HA, Lee SM, Park S, Rhee SG. Characterization of mammalian sulfiredoxin and its reactivation of hyperoxidized peroxiredoxin through reduction of cysteine sulfinic acid in the active site to cysteine. J Biol Chem 2004;279:50994–51001.
[38] Woo HA, Jeong W, Chang TS, Park KJ, Park SJ, Yang JS, Rhee SG. Reduction of cysteine sulfinic acid by sulfiredoxin is specific to 2-cys peroxiredoxins. J Biol Chem 2005;280:3125–3128.
[39] Lazebnik YA, Kaufmann SH, Desnoyers S, Poirier GG, Earnshaw WC. Cleavage of poly(ADP-ribose) polymerase by a proteinase with properties like ICE. Nature 1994; 371:346–347.
[40] Hishita T, Tada-Oikawa S, Tohyama K, Miura Y, Nishihara T, Tohyama Y, Yoshida Y, Uchiyama T, Kawanishi S. Caspase-3 activation by lysosomal enzymes in cytochrome *c*-independent apoptosis in myelodysplastic syndrome-derived cell line P39. Cancer Res 2001;61:2878–2884.